

Brownian motion in confinement

Thorben Benesch* and Sotira Yiacoymi†

Georgia Institute of Technology, 311 Ferst Drive, Atlanta, Georgia 30332-0512, USA

Costas Tsouris

Oak Ridge National Laboratory, P.O. Box 2008, Oak Ridge, Tennessee 37831-6181, USA

(Received 25 March 2003; published 5 August 2003)

This research modifies an earlier approach based on the single-wall reflection method to predict the perpendicular and parallel diffusion coefficients of a Brownian sphere in confinement. The modified version provides predictions that match experimental data reported in the literature more accurately than those provided by other available models, including the linear superposition approximation, the coherent superposition approximation, and Oseen's equation.

DOI: 10.1103/PhysRevE.68.021401

PACS number(s): 82.70.-y, 95.30.Lz, 81.05.-t, 81.05.Rm

I. INTRODUCTION

Although the first investigations concerning confined Brownian motion were performed a long time ago [1], this problem remains the subject of discussions [2,3]. The importance of understanding the motion of spheres in confinement lies in its applicability to the description of particles migrating in porous media or near fluid-solid boundaries, macromolecules diffusing in membranes, and cells interacting with surfaces [4,5]. In addition to the influence of the wall on the Brownian motion of particles, the hydrodynamic coupling of two colloidal spheres through a boundary has been found to affect attractive interaction of the spheres [6,7].

Recent advances in information processing power and image processing by means of dynamic-light-scattering techniques [8], video microscopy [4,9], and digital imaging [10], as well as controlled manipulation of colloidal spheres through optical tweezers [11,12], have provided new insight into the influence of walls on the diffusion coefficient.

While the influence of a wall on the motion of a sphere may be solved mathematically [1], the effect of a second boundary is still an open question. In 1923, Faxén developed formulas describing the effects of a single wall on the motion of a sphere and expanded these formulas to describe highly symmetric arrangements of two walls. Oseen suggested that the effects of two single walls be added, deriving the following equation [1]:

$$\frac{D_{\parallel}^{\text{II}}}{D_0} = 1 - \frac{9a}{16} \left(\frac{1}{z} + \frac{1}{d-z} \right), \quad (1a)$$

where a is the radius of the sphere, d is the width of the gap, z is the center of the sphere-to-wall distance, and $D_{\parallel}^{\text{II}}$ is the parallel diffusion in confinement. Using the analogous expression for the motion of a sphere perpendicular to a single wall (D_{\perp}^{I}) [1], Oseen's equation, Eq. (1a), originally derived

for parallel diffusion, may be adapted for perpendicular diffusion in confinement (D_{\perp}^{II}), as shown by Eq. (1b),

$$\frac{D_{\perp}^{\text{II}}}{D_0} = 1 - \frac{9a}{8} \left(\frac{1}{z} + \frac{1}{d-z} \right). \quad (1b)$$

In the equations above, the diffusion coefficient in free space, D_0 , is given by the Stokes-Einstein formula

$$D_0 = \frac{kT}{6\pi\eta a}, \quad (2)$$

where k is the Boltzmann constant, T is the absolute temperature, and η is the viscosity of the fluid.

Integrating the solution of Liron and Mochon [13], who employed Blake's treatment for the stokeslet in a no-slip boundary [14], one obtains an accurate but unwieldy solution [9]. Dufresne, Altman, and Grier [9] obtained a solution for cases in which the far-field contribution dominates the flow at the boundary (i.e., where the radius is much smaller than the width). Through extension of the single-wall reflection, Lobry and Ostrowsky [8] derived the diffusion coefficient in confinement that includes multiple reflections, which is given by

$$\begin{aligned} \frac{D^{\text{II}}}{D_0} = & \left\{ 1 + \sum_{n=0}^{\infty} \left[\frac{D_0}{D^{\text{I}}(nd+z)} - 1 \right] \right. \\ & + \sum_{n=0}^{\infty} \left[\frac{D_0}{D^{\text{I}}((n+1)d-z)} - 1 \right] \\ & \left. - 2 \sum_{n=1}^{\infty} \left[\frac{D_0}{D^{\text{I}}(nd)} - 1 \right] + O\left(\frac{a}{d}\right)^2 \right\}^{-1}. \quad (3) \end{aligned}$$

Here, the diffusion coefficient D^{II} for two walls represents both cases, the perpendicular (D_{\perp}^{II}) and parallel ($D_{\parallel}^{\text{II}}$) diffusion in confinement, and depends on the diffusion coefficient in free space D_0 , as defined by Eq. (3), and the diffusion coefficient for the single wall D^{I} , which is given by Eq. (4a) for perpendicular (D_{\perp}^{I}) and Eq. (4b) for parallel (D_{\parallel}^{I}) diffusion:

*Present address: BASF AG, Global Engineering, Ludwigshafen, Germany. Email address: Thorben.Benesch@basf-ag.de

†Corresponding author. FAX: (404) 894-8266. Email address: syiacourni@ce.gatech.edu

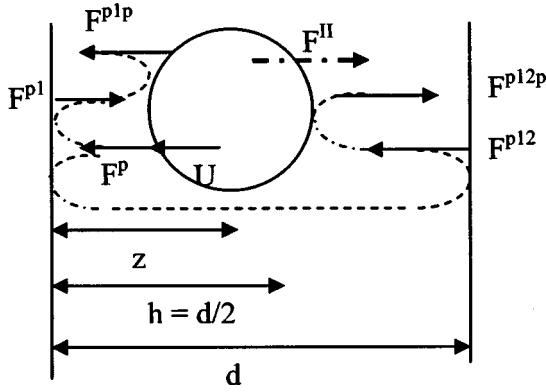


FIG. 1. Motion of a sphere in confinement. The velocity fields as well as the reflections of n th order are reflected at the left and right boundaries and at the sphere.

$$\frac{D_{\perp}^I(u)}{D_0} = 1 - \frac{9a}{8(u)} \quad (4a)$$

and

$$\frac{D_{\parallel}^I(u)}{D_0} = 1 - \frac{9a}{16(u)}. \quad (4b)$$

The variable u is used as a general transformation of $nd + z$, $(n+1)d - z$, and nd . In this work, the model of Lobry and Ostrowsky [8] is referred to as coherent superposition assumption (CSA), as introduced by Lin, Yu, and Rice [4]. These researchers showed the CSA to be less accurate than the linear superposition approximation (LSA) adopted by Fauchaux and Libchaber [10] and given by Eq. (5):

$$\frac{D^{\text{II}}}{D_0} = \left\{ 1 + \left[\frac{D_0}{D^I(z)} - 1 \right] + \left[\frac{D_0}{D^I(d-z)} - 1 \right] \right\}^{-1}. \quad (5)$$

As before, Eq. (5) may be applied for either case, the perpendicular (D_{\perp}^{II}) or parallel ($D_{\parallel}^{\text{II}}$) diffusion in confinement, if Eq. (4a) or (4b) is, respectively, inserted for D^I and Eq. (3) is inserted for D_0 . The LSA, however, violates boundary conditions at both bounding surfaces [9]. Note that the drag force F^{II} and the diffusion coefficient D^{II} are related by $F^{\text{II}}/F_0 = D_0/D^{\text{II}}$, so that similar equations may be derived for the drag force. Both quantities have been used extensively in the literature [1,4,8,9,15]. This paper deals exclusively with the diffusion coefficient, since all available experimental data are in terms of this quantity. We revisited the experiments of Refs. [4,8], and compared Oseen's solution, the LSA, and the CSA with a modified CSA (MCSA) solution [16].

II. DERIVATION OF THE MODIFIED COHERENT SUPERPOSITION APPROXIMATION

The diffusion coefficient for a sphere in confinement is derived by analogy to Lobry and Ostrowsky [8], using the method of reflections and assuming the motion of the sphere as a point force ("stokeslet") shown in Fig. 1. The complete

force is the sum of the point force and the reflections of n th order:

$$F^{\text{II}} = F^p + F^{p1p} + F^{p2p} + F^{p12p} + F^{p21p} + \dots \quad (6)$$

One can express the reflections by the single-wall reflections F^I , which are given by Eq. (4) when the relation $F/F_0 = D_0/D$ is used:

$$F^{p1p} = F^I(z) - F_0, \quad F^{p2p} = F^I(d-z) - F_0,$$

$$F^{p12p} = -F^I(2d-z) + F_0, \quad F^{p21p} = -F^I(d+z) + F_0,$$

$$F^{p121p} = F^I(2d+z) - F_0, \quad F^{p212p} = F^I(3d-z) - F_0,$$

$$F^{p1212p} = -F^I(4d-z) + F_0,$$

and

$$F^{p2121p} = -F^I(3d+z) + F_0. \quad (7)$$

The significant difference between the CSA and the MCSA is the consideration of the sphere-wall distance in the higher-order terms. In Ref. [8], the second reflections (F^{p12p} and F^{p21p}) are taken into account as a particle placed at a distance d away from the original particle, the third reflections (i.e., F^{p121p} and F^{p212p}) as a particle placed at a distance $z+d$ away from the original particle, etc. Thus, one obtains three series, as shown in Eq. (3), in which the first accounts for the odd reflections on the wall that is placed at a distance z away from the sphere, the second accounts for the odd reflections on the opposite side, and the third sums the even reflections. In the MCSA, the first reflections are analogous to those of the CSA. However, it is assumed that after being reflected at the first wall, the velocity field spreads over the distance d between the two walls and then is reflected at the second wall and spreads over the distance $d - z$. Thus, the second reflection is considered as a reflection of the motion of a sphere that is placed a distance $2d - z$ away from the wall. Analogously, the second reflection of the opposite wall is considered as the reflection of a sphere placed at distance $d + z$, as given by Eq. (7). The higher-order reflections, up to the fourth, are derived in an analogous way [16]. Therefore, the total force is given by

$$F^{\text{II}} = F_0 + \sum_{n=0}^{\infty} (-1)^n [F^I(nd+z) - F_0] + \sum_{n=0}^{\infty} (-1)^n [F^I((n+1)d-z) - F_0] + O\left(\frac{a}{d}\right)^2. \quad (8)$$

In order to be comparable to Eqs. (1), (3), and (5), Eq. (8) must be written in terms of diffusion coefficients through the relation $F/F_0 = D_0/D$:

$$\frac{D^{\text{II}}}{D_0} = \left\{ 1 + \sum_{n=0}^{\infty} (-1)^n \left[\frac{D_0}{D^I(nd+z)} - 1 \right] + \sum_{n=0}^{\infty} (-1)^n \left[\frac{D_0}{D^I((n+1)d-z)} - 1 \right] \right\}^{-1}. \quad (9)$$

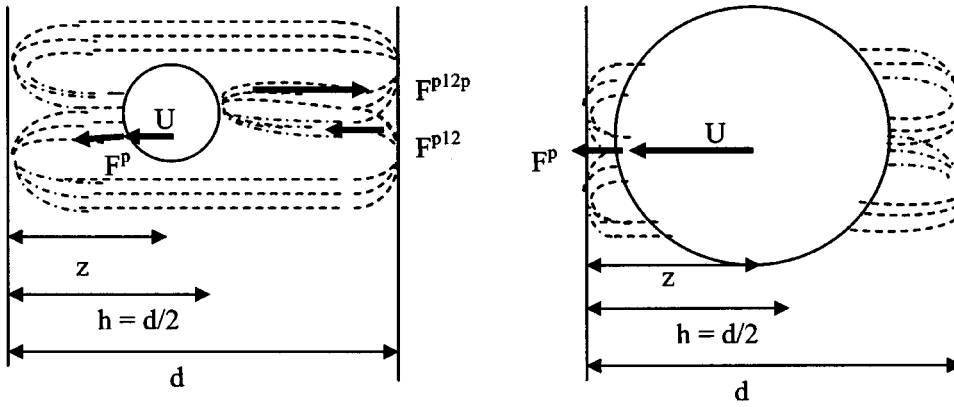


FIG. 2. Motion of a small sphere and a large sphere in confinement. The larger the sphere, the less possible are higher-order reflections.

By using Eq. (4a) or (4b) for D^I , Eq. (9) may apply for perpendicular (D^I_{\perp}) or parallel (D^I_{\parallel}) diffusion in confinement.

Noting that the results of Lin, Yu, and Rice [4] show that the higher-order terms are more relevant for larger h/a ratios (i.e., small spheres in wide gaps with half-width h), while the motion of a sphere in a small gap can be better described by the LSA, one may assume that not the center-of-sphere-to-wall distance, but the shortest sphere-to-wall distance determines the diffusion in confinement. Figure 2 emphasizes that the sphere is a resistance that hinders the reflected waves from crossing the whole gap. Thus, the influence of the higher-order reflections diminishes with increasing sphere diameter. This effect cannot be described by Eq. (9), since the equation is derived for a point force. To account for the finite size of the sphere, empirical factors need to be introduced that set the shortest distance of the sphere to wall into relation with the distance of the stokeslet as shown in Fig. 3. The second-order reflections are reduced by the ratio between the shortest sphere-to-wall distances and the center-of-sphere-to-wall distances $(z-a)/z$ and $(2h-z-a)/(2h-z)$, and third-order reflections F^{p121p} and F^{p212p} are reduced by the factors

$(2h+z-a)/(2h+z)$ and $(4h-z-a)/(4h-z)$. In the same way, the n th-order reflections are reduced by $[2(n-1)h+z-a]/[2(n+1)h+z]$ and $(2nh-z-a)/(2nh-z)$, respectively.

On one hand, the higher-order terms become negligible as $h/a \rightarrow 1$, while on the other hand, Eq. (10) gives the theoretical derivation, i.e., Eq. (9), as $a \rightarrow 0$:

$$\begin{aligned} \frac{D^{\text{II}}}{D_0} = & \left\{ 1 + \left[\frac{D_0}{D^I(z)} - 1 \right] + \left[\frac{D_0}{D^I(2h-z)} - 1 \right] \right. \\ & + \sum_{n=1}^{\infty} (-1)^n \frac{2nh-z-a}{2nh-z} \left[\frac{D_0}{D^I(2nh+z)} - 1 \right] \\ & + \sum_{n=1}^{\infty} (-1)^n \frac{(n-1)2h+z-a}{(n-1)2h+z} \\ & \left. \times \left[\frac{D_0}{D^I(2(n+1)h-z)} - 1 \right] \right\}^{-1}. \end{aligned} \quad (10)$$

The variables D^I , D^{II} , and D_0 are used in analogy to Eqs.

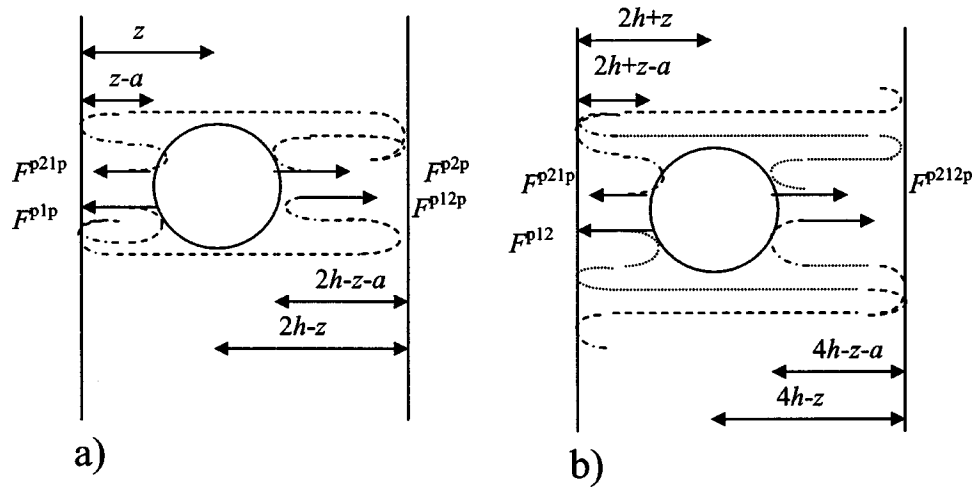


FIG. 3. Reduction of the higher-order reflections through the finite size of the sphere. In (a), one can see the first-order reflections F^{p1p} and F^{p2p} and the second-order reflections F^{p12p} and F^{p21p} ; the waves that are reflected on the wall may hit the sphere or reflect again on the opposite wall. The larger the radius a , the less the chance is for the wave to pass the sphere. The second reflections are reduced by the ratio between the shortest sphere-to-wall distances and the center-of-sphere-to-wall distances $(z-a)/z$ and $(2h-z-a)/(2h-z)$. Because of the same reason, the third-order reflections F^{p121p} and F^{p212p} are reduced by the factors $(2h+z-a)/(2h+z)$ and $(4h-z-a)/(4h-z)$.

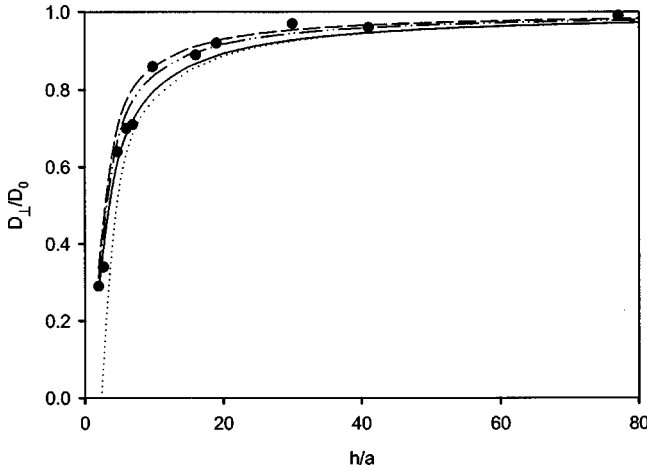


FIG. 4. Perpendicular diffusion coefficient of a sphere that is placed at $z=h$ as a function of the half-width h of the gap. The influence becomes negligible for gaps with half-widths that are 20 times larger than the radius. Solid line, LSA; dotted line, Oseen's equation; short-dashed line, CSA; dashed-dotted line, MCSA; solid dots, experiments of Lin, Yu, and Rice (Ref. [4]).

(3), (5), and (9) and may be adapted in the same way for perpendicular (D_{\perp}) or parallel diffusion (D_{\parallel}). The width d is replaced by the half-width h , i.e., $d=2h$.

III. RESULTS

The computations and measurements of Lin, Yu, and Rice [4] for the perpendicular diffusion coefficient of a sphere placed at the midplane h of a gap are shown in Fig. 4. The equations used in the computations of Fig. 4, as well as Figs. 5 and 6, are listed in Table I. The comparison of the models in Fig. 4 shows that the MCSA predicts the experimental data of Lin, Yu, and Rice [4] for the perpendicular diffusion much better than the CSA. The variance σ^2 given by Eq. (11) is 1.48×10^{-3} for the MCSA, 4.31×10^{-3} for the CSA,

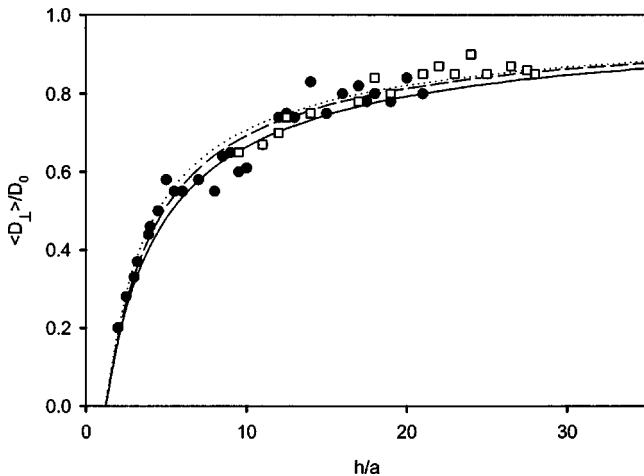


FIG. 5. Average perpendicular diffusion coefficient in a comparison of three models with experimental data taken from Ref. [8]. The spheres fluctuate between $z=a$ and $z=h$. Solid line, LSA; dotted line, CSA; short-dashed line, MCSA; solid dots, experiments ($a=0.11 \mu\text{m}$); open squares, experiments ($a=0.039 \mu\text{m}$).

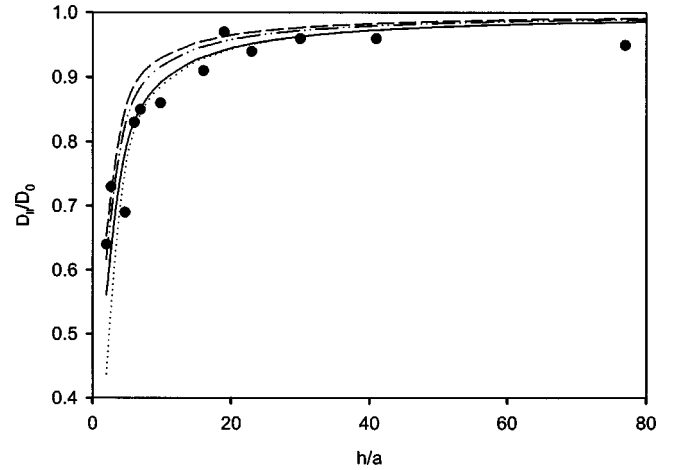


FIG. 6. Parallel diffusion coefficient of a sphere that is placed at $z=h$ as a function of the half-width h of the gap. The influence becomes negligible for gaps with half-widths that are 20 times larger than the radius. Solid line, LSA; dotted line, Oseen's equation; short-dashed line, CSA; dashed-dotted line, MCSA; solid dots, experiments of Lin, Yu, and Rice (Ref. [4]).

1.44×10^{-3} for the LSA, and 2.36×10^{-2} for Oseen's equation:

$$\sigma^2 = \frac{1}{(N-1)D_0^2} \sum_{n=1}^N (D_{\text{expt}}^{\text{II}} - D_{\text{model}}^{\text{II}})^2. \quad (11)$$

Note that the largest error results from the second experimental point. Excluding this point yields a σ^2 of 5.77×10^{-4} for the MCSA, which is more accurate than a σ^2 of 1.03×10^{-3} for the LSA.

If the particle is free to move perpendicular to the wall, it will be located at any distance z from the wall that is between the radius of the sphere a and the gap half-width $h=d/2$. To account for these fluctuations, Lobry and Ostrowsky [8] measured the average diffusion coefficient. Therefore, Eqs. (3), (5), and (10) have to be averaged in order to be comparable with the experimental data of Ref. [8]:

$$\langle D^{\text{II}} \rangle = \frac{\int_a^h D^{\text{II}}(z, h) dz}{\int_a^h dz}, \quad (12)$$

where $D^{\text{II}}(z, h)$ is the parallel or perpendicular diffusion coefficient given by Eqs. (3), (5), and (10), respectively.

The integral of Eq. (12) has been solved numerically by means of the Monte Carlo simulation. The values are obtained from 100 000 random steps that are required for a smooth line:

$$\left\langle D\left(\frac{h}{a}\right) \right\rangle = \frac{\sum_{i=1}^N D\left[R(i)\left(\frac{h}{a}-1\right)+1\right]}{N}, \quad (13)$$

where $R(i)$ is a random number between 0 and 1 and N is the number of random steps.

TABLE I. Models used for the computations shown in Figs. 4–6.

Model	Geometry	Perpendicular diffusion	Parallel diffusion
	Single wall	Eqs. (2) and (4a)	Eqs. (2) and (4b)
Oseen	Double wall	Eqs. (1b) and (2)	Eqs. (1a) and (2)
CSA	Double wall	Eqs. (2), (3), and (4a)	Eqs. (2), (3), and (4b)
LSA	Double wall	Eqs. (2), (5), and (4a)	Eqs. (2), (5), and (4b)
MCSA	Double wall	Eqs. (2), (10), and (4a)	Eqs. (2), (10), and (4b)

Figure 5 shows that the average diffusion coefficient is smaller than the diffusion coefficient at the midplane h . Furthermore, one can see that the values predicted by the MCSA are between those predicted by the LSA and the CSA models. A comparison with the experimental data of Ref. [8] shows that the model of this work predicts the experiments more accurately than the other models. For the larger sphere (i.e., $a=0.11\ \mu\text{m}$), values of σ^2 are 1.52×10^{-3} , 2.01×10^{-3} , and 1.95×10^{-3} for the MCSA, the CSA, and the LSA, respectively. For the smaller sphere (i.e., $a=0.039\ \mu\text{m}$), σ^2 is 8.99×10^{-4} , 9.45×10^{-4} , and 1.55×10^{-3} for the MCSA, the CSA, and the LSA, respectively. Therefore, the MCSA more accurately predicts the experimental data of Ref. [8].

Figure 6 compares the theoretical predictions obtained for the parallel diffusion of a sphere placed at the midplane h by Oseen's equation, the LSA, the CSA, and the MCSA with the experimental data of Ref. [4]. Analogous to the previous results, the influence of confinement on the parallel diffusion coefficient diminishes in wide gaps. With a variance of 2.72×10^{-3} , the MCSA matches better with the experiments of Lin, Yu, and Rice [4] than does the CSA approximation, which has a σ^2 of 3.87×10^{-3} , or Oseen's equation, which has a σ^2 of 6.49×10^{-3} . However, with a σ^2 of 2.27×10^{-3} , the prediction of the LSA is still better than that of the MCSA. The fact that Ref. [4] reports only 12 data points, however, suggests that more experimental data are needed for a better comparison. As for the perpendicular diffusion, also in this measurement, one data point is very inaccurate. Excluding this point yields a σ^2 of 1.36×10^{-3} for the MCSA, which is more accurate than a σ^2 of 1.57×10^{-3} for the LSA.

IV. CONCLUSION AND SUMMARY

In this work, an equation based on the method of reflection has been used for the computation of the perpendicular and parallel diffusion coefficients in confinement. This equation, a modification of the coherent superposition approximation (CSA), is referred to as the MCSA. Computations using the MCSA have shown that the higher-order reflections are less relevant when large spheres are suspended in small gaps. Furthermore, the reflection at the close wall dominates if the sphere is placed asymmetrically in the gap. These effects may be explained by the fact that the motion of a sphere depends on the distance between the surface of the sphere and the wall and that higher-order reflections are hindered by large spheres. An additional factor in the MCSA corrects the failure in describing the motion of a sphere with finite size by means of a stokeslet. Therefore, reflections on the opposite site are negligible if $d-z-a\gg z-a$, and higher-order reflections are negligible for $h/a\rightarrow 1$. Comparisons of various models with the experimental data of Lin, Yu, and Rice [4] and Lobry and Ostrowsky [8] have shown that the MCSA predicts perpendicular as well as parallel diffusion better than other existing models.

ACKNOWLEDGMENTS

Partial support for this research was provided by the National Science Foundation (Grant No. BES-9702356 to S.Y.), and by the Division of Chemical Sciences, Office of Basic Energy Sciences, U.S. Department of Energy, under Contract No. DE-AC05-00OR22725 with UT-Battelle, LLC. The authors are also thankful to Dr. Marsha K. Savage for editing the manuscript.

-
- [1] J. Happel and H. Brenner, *Low Reynolds Number Hydrodynamics* (Prentice-Hall, Englewood Cliffs, NJ, 1965).
 - [2] P. Lancon, G. Batrouni, L. Lobry, and N. Ostrowsky, *Europhys. Lett.* **54**, 23 (2001).
 - [3] P. Lancon, G. Batrouni, L. Lobry, and N. Ostrowsky, *Physica A* **304**, 65 (2002).
 - [4] B. Lin, J. Yu, and S. A. Rice, *Phys. Rev. E* **62**, 3909 (2000).
 - [5] W. B. Russel, D. A. Saville, and W. R. Schowalter, *Colloidal Dispersion* (Cambridge University Press, Cambridge, 1989).
 - [6] T. M. Squires and M. P. Brenner, *Phys. Rev. Lett.* **85**, 4976 (2002).
 - [7] T. Benesch, S. Yiacoumi, and C. Tsouris (unpublished).
 - [8] L. Lobry and N. Ostrowsky, *Phys. Rev. B* **53**, 12 050 (1996).
 - [9] E. R. Dufresne, D. Altman, and D. G. Grier, *Europhys. Lett.* **53**, 264 (2001).
 - [10] L. P. Faucheux and A. J. Libchaber, *Phys. Rev. E* **49**, 5158 (1994).
 - [11] A. Ashkin, J. M. Dziedzic, J. E. Bjorkholm, and S. Chu, *Opt. Lett.* **11**, 288 (1986).
 - [12] D. G. Grier, *Curr. Opin. Colloid Interface Sci.* **2**, 264 (1997).
 - [13] N. Liron and S. Mochon, *J. Eng. Math.* **10**, 287 (1976).
 - [14] J. R. Blake, *Proc. Cambridge Philos. Soc.* **70**, 303 (1971).
 - [15] E. R. Dufresne, T. M. Squires, M. P. Brenner, and D. G. Grier, *Phys. Rev. Lett.* **85**, 3317 (2000).
 - [16] T. Benesch, master's thesis, Georgia Institute of Technology, Atlanta, GA, 2002.